Chapter 5

Light Wave Propagation and Scattering Through Particles

Yi Ping Han, Zhi Wei Cui and Jia Jie Wang

Additional information is available at the end of the chapter

http://dx.doi.org/10.5772/66662

Abstract

The study of light propagating and scattering for various particles has always been important in many practical applications, such as optical diagnostics for combustion, monitoring of atmospheric pollution, analysis of the structure and pathological changes of the biological cell, laser Doppler technology, and so on. This chapter discusses propagation and scattering through particles. The description of the solution methods, numerical results, and potential application of the light scattering by typical particles is introduced. The generalized Lorenz-Mie theory (GLMT) for solving the problem of Gaussian laser beam scattering by typical particles with regular shapes, including spherical particles, spheroidal particles, and cylindrical particles, is described. The numerical methods for the scattering of Gaussian laser beam by complex particles with arbitrarily shape and structure, as well as random discrete particles are introduced. The essential formulations of numerical methods are outlined, and the numerical results for some complex particles are also presented.

Keywords: light scattering, small particles, Gaussian laser beam, generalized Loren-Mie theory, numerical method

1. Introduction

The investigation of light propagation and scattering by various complex particles is of great importance in a wide range of scientific fields, and it has lots of practical applications, such as detection of atmospheric pollution, optical diagnostics for aerosols, remote sensing of disasters [1–3]. Over the past few decades, some theories and numerical methods have been developed to study the light wave propagation and scattering through various particles. For the particles with special shape, such as spheres, spheroids, and cylinders, the generalized Lorenz-Mie theory (GLMT) [4–15] can obtain an analytic solution in terms of a limited linear system of equations using the method of separation of variables to solve the Helmholtz equation in the corresponding coordinate system. For the complex particles of arbitrary shapes and structure, some numerical methods, such as the discrete dipole approximation (DDA), the method of moments (MOM), the finite element method (FEM), and the finite-difference time-domain (FDTD), have been utilized. For random media composed of many discrete particles, the T-matrix method, the sparse-matrix canonical-grid (SMCG) method, and the characteristic basis function method (CBFM) can be applied to obtain simulation results.

This chapter discusses the light propagation and scattering through particles. Without loss of generality, the incident light is assumed to be Gaussian laser beam, which can be reduced to conventional plane wave. The detailed description of the solution methods, numerical results, and potential application of the light scattering by systems of particles is introduced.

2. Light scattering by regular particles

2.1. Light scattering by a homogeneous sphere

The geometry of light scattering of a Gaussian beam by a homogeneous sphere is illustrated in **Figure 1**. As shown in **Figure 1**, two Cartesian coordinates $Oxyz$ and $O_b uvw$ are used. The $Oxyz$ is attached to the particle whose center is located at O, and the $O_b uvw$ is attached to the shaped beam. Due to the spherical symmetry of the homogeneous sphere, it is common to assume that the axes $O_b u$, $O_b v$, and $O_b w$ are parallel to the axes Ox, Oy, and Oz, respectively. The shaped

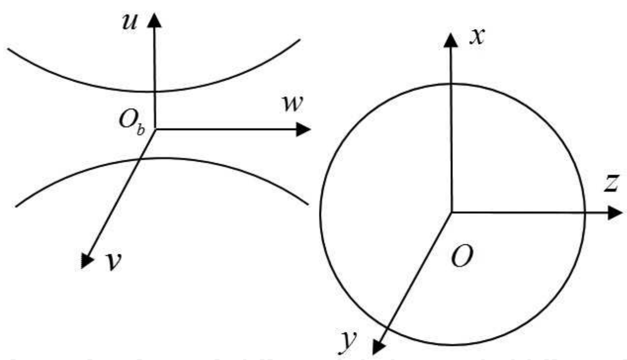

Figure 1. Geometry of the scattering of a Gaussian beam by a homogeneous sphere.

beam is assumed to be propagating along the positive w-axis of the beam system, with its electric field polarized along the u-axis. The time-dependent part of the electromagnetic fields is $\exp(-i\omega t)$, which will be omitted throughout this section.

Within the framework of the GLMT, the electromagnetic field components of the illuminating beam are described by partial wave expansions over a set of basic functions, e.g., vector spherical wave functions in spherical coordinates, vector spheroidal wave functions in spheroidal coordinates, and vector cylindrical wave functions in cylindrical coordinates. The expansion coefficients or sub-coefficients are named as beam-shape coefficients (BSCs) are denoted as $g_{n,X}^m$

(X is TE, transverse electric, or TM, transverse magnetic, with n from 1 to ∞, m from $-n$ to n). Considering the scattering of a spherical particle, the incident Gaussian beam can be expanded in terms of vector spherical wave functions in the particle coordinate system $Oxyz$ as

$$\mathbf{E}^i = E_0 \sum_{n=1}^{\infty} \sum_{m=-n}^{n} C_{nm} \left[i g_{n,TE}^m \mathbf{m}_{mn}^{(1)}(kR,\theta,\varphi) + g_{n,TM}^m \mathbf{n}_{mn}^{(1)}(kR,\theta,\varphi) \right] \tag{1}$$

$$\mathbf{H}^i = E_0 \frac{k}{\omega\mu} \sum_{n=1}^{\infty} \sum_{m=-n}^{n} C_{nm} \left[g_{n,TE}^m \mathbf{n}_{mn}^{(1)}(kR,\theta,\varphi) - i g_{n,TM}^m \mathbf{m}_{mn}^{(1)}(kR,\theta,\varphi) \right] \tag{2}$$

where the superscript "i" indicates "incident". The C_{nm} is a constant with explicit expression

$$C_{nm} = (-1)^{(m-|m|)/2} \frac{(n-m)!}{(n-|m|)!} i^{n-1} \frac{2n+1}{n(n+1)}. \tag{3}$$

The $\mathbf{m}_{mn}^{(j)} = \mathbf{m}_{emn}^{(j)} + i\mathbf{m}_{omn}^{(j)}$ and $\mathbf{n}_{mn}^{(j)} = \mathbf{n}_{emn}^{(j)} + i\mathbf{n}_{omn}^{(j)}$ are the vector spherical wave functions with detailed expressions

$$\begin{bmatrix} \mathbf{m}_{emn}^{(j)} \\ \mathbf{m}_{omn}^{(j)} \end{bmatrix} = m\pi_n^m(\cos\theta)\, z_n^{(j)}(kR) \begin{bmatrix} -\sin m\varphi \\ \cos m\varphi \end{bmatrix} \mathbf{e}_\theta - z_n^{(j)}(kR)\tau_n^m(\cos\theta) \begin{bmatrix} \cos m\varphi \\ \sin m\varphi \end{bmatrix} \mathbf{e}_\varphi \tag{4}$$

$$\begin{bmatrix} \mathbf{n}_{emn}^{(j)} \\ \mathbf{n}_{omn}^{(j)} \end{bmatrix} = \left\{ z_n^{(j)}(kR) n(n+1) P_n^m(\cos\theta) \begin{bmatrix} \cos m\varphi \\ \sin m\varphi \end{bmatrix} \mathbf{e}_R + \frac{d\left[kR z_n^{(j)}(kR)\right]}{d(kR)} \tau_n^m(\cos\theta) \begin{bmatrix} \cos m\varphi \\ \sin m\varphi \end{bmatrix} \mathbf{e}_\theta \right.$$
$$\left. + \frac{d[kR z_n^{(j)}(kR)]}{d(kR)} m\pi_n^m(\cos\theta) \begin{bmatrix} -\sin m\varphi \\ \cos m\varphi \end{bmatrix} \mathbf{e}_\varphi \right\} \cdot \frac{1}{kR} \tag{5}$$

the index corresponds to the spherical Bessel functions of the first, second, third, or fourth kind ($j = 1, 2, 3, 4$). The angular functions $\pi_n^m(cos\theta)$ and $\tau_n^m(cos\theta)$ are defined as

$$\pi_n^m(cos\theta) = \frac{P_n^m(cos\theta)}{\sin\theta}, \tau_n^m(cos\theta) = \frac{d}{d\theta} P_n^m(cos\theta). \tag{6}$$

The electric component of the internal field and the scattered field can be expanded in terms of vector spherical wave functions in the particle coordinate system $Oxyz$, respectively, as

$$\mathbf{E}^{int} = E_0 \sum_{n=1}^{\infty} \sum_{m=-n}^{n} \left[f_{mn} \mathbf{m}_{mn}^{(1)}(kR,\theta,\varphi) + g_{mn} \mathbf{n}_{mn}^{(1)}(kR,\theta,\varphi) \right] \tag{7}$$

$$\mathbf{E}^{sca} = E_0 \sum_{n=1}^{\infty} \sum_{m=-n}^{n} \left[a_{mn} \mathbf{m}_{mn}^{(3)}(kR,\theta,\varphi) + b_{mn} \mathbf{n}_{mn}^{(3)}(kR,\theta,\varphi) \right]. \tag{8}$$

To solve the scattering problem, light scattering, the scattering coefficients a_{mn} and b_{mn} are then determined by applying the tangential continuity of the electric and magnetic fields at the surface of the sphere

$$a_{mn} = a_n \cdot g^m_{n,TM}, b_{mn} = b_n \cdot g^m_{n,TM} \tag{9}$$

where a_n, b_n are the classical scattering coefficients of the Lorenz-Mie theory as

$$a_n = \frac{\psi_n(x)\psi'_n(Mx) - M\psi'_n(x)\psi_n(Mx)}{\xi^{(1)}_n(x)\psi'_n(Mx) - M\xi'^{(1)}_n(x)\psi_n(Mx)} \tag{10}$$

$$b_n = \frac{M\psi_n(x)\psi'_n(Mx) - \psi_n(Mx)\psi'_n(x)}{M\xi^{(1)}_n(x)\psi'_n(Mx) - \xi'^{(1)}_n(x)\psi_n(Mx)} \tag{11}$$

where $M = k/k_0$. Once the obtained scattering coefficients are determined, the far-zone scattered field E^{sca}_{far} can be obtained, and the differential scattering cross section (DSCS) of particles can be calculated by

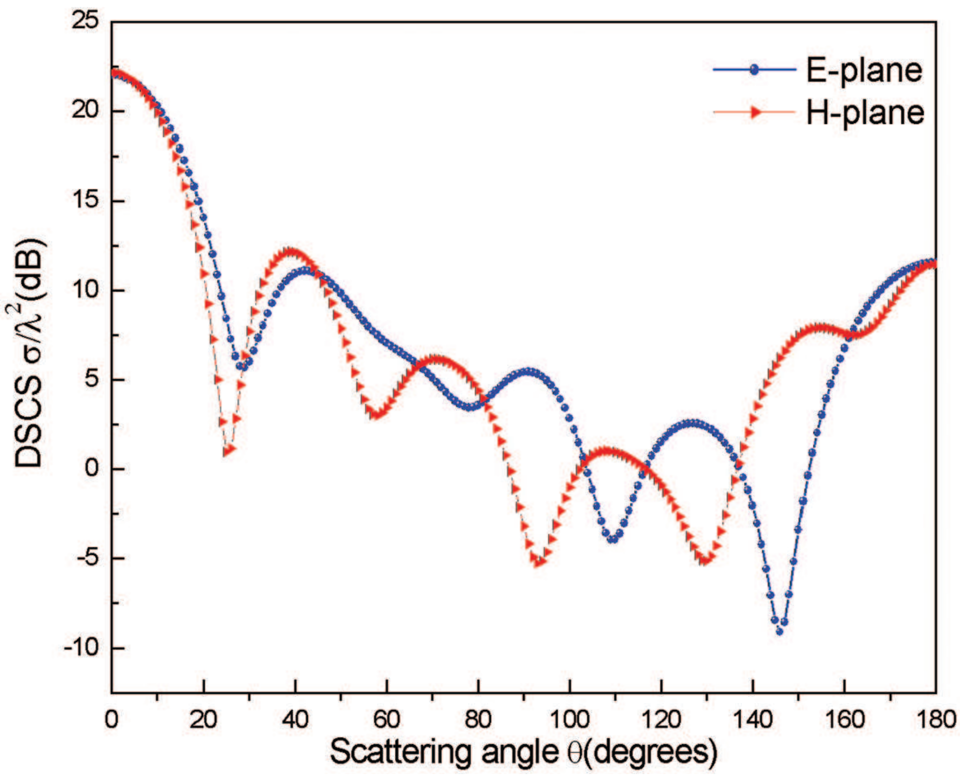

Figure 2. DSCS for a homogeneous spherical dielectric particle illuminated by a Gaussian beam.

$$\sigma(\theta, \varphi) = \lim_{r \to \infty} 4\pi r^2 |E^{sca}_{far}/E_0|^2. \tag{12}$$

Figure 2 presents the normalized DSCS for the scattering of a Gaussian beam by a homogeneous spherical dielectric particle. The radius of the spherical particle is $r = 1.0\lambda$, and the refractive index of the particle is $m = 2.0$. The beam center is located at the origin of the particle system with beam waist radius of $\omega_0 = 2\lambda$, and the angle set of the beam is $\alpha = \beta = \gamma = 0^o$.

2.2. Light scattering by a spheroidal particle

Light scattering by a spheroid has been of great interest to many researchers in the past several decades since it provides an appropriate model in many practical situations. For example, during the atomization processes, the shape of fuel droplets departs from sphere to spheroid when it impinges on the wall and breaks. Due to the inertial force, the raindrop also departs from the spherical particle to the near-spheroidal one. A rigorous solution to the scattering problem concerning a homogeneous spheroid illuminated by a plane wave was first derived by Asano and Yamamoto [16]. It was extended later to the cases of shaped beam illumination [17], a layered spheroid [18], and a spheroid with an embedded source [19]. Nevertheless, only parallel incident of the shaped beam, including on-axis and off-axis Gaussian beam scattered by a spheroid was studied, that is to say, the propagation direction of the incident beam is assumed to be parallel to the symmetry axis of the spheroid. An extension of shaped beam scattering with arbitrary incidence was developed within the framework of GLMT by Han et al. [20–22] and Xu et al. [23, 24].

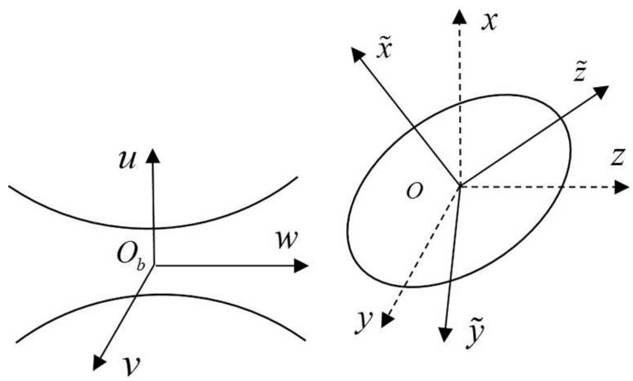

Figure 3. Geometry of a prolate spheroid illuminated by a shaped beam.

To deal with the shaped beam scattering of a spheroidal particle within the framework of GLMT, the incident Gaussian beam is required to be expanded in terms of the vector spheroidal wave functions in spheroidal coordinates, which can be achieved using the relationship between the vector spherical wave functions and the spherical wave functions. The geometry of shaped beam scattering by a prolate spheroid is illustrated in **Figure 3**. According to the expansion of shaped beam in unrotated spherical coordinates in Eq. (1), we can rewrite it as

$$\begin{aligned}\mathbf{E}^{inc} = E_0 \sum_{n=1}^{\infty} \sum_{m=0}^{n} [\overline{g_{n,TE}^{m}} \mathbf{m}_{emn}^{r(1)}(kR,\theta,\varphi) + \overline{g_{n,TE}^{\prime m}} \mathbf{m}_{omn}^{r(1)}(kR,\theta,\varphi) \\ + i\overline{g_{n,TM}^{\prime m}} \mathbf{n}_{emn}^{r(1)}(kR,\theta,\varphi) + i\overline{g_{n,TM}^{m}} \mathbf{n}_{omn}^{r(1)}(kR,\theta,\varphi)]\end{aligned} \tag{13}$$

where we have

$$\begin{pmatrix} \overline{g^{m}_{n,TE}} \\ \overline{g'^{m}_{n,TE}} \\ \overline{g^{m}_{n,TM}} \\ \overline{g'^{m}_{n,TM}} \end{pmatrix} = i^{n} \frac{2n+1}{n(n+1)} \frac{1}{(1+\delta_{0m})} \begin{pmatrix} 1 \\ i \\ -i \\ -1 \end{pmatrix} \begin{pmatrix} (g^{m}_{n,TE} + g^{-m}_{n,TE}) \\ (g^{m}_{n,TE} - g^{-m}_{n,TE}) \\ (g^{m}_{n,TM} - g^{-m}_{n,TM}) \\ (g^{m}_{n,TM} + g^{-m}_{n,TM}) \end{pmatrix} \tag{14}$$

where δ_{0m} is the Kronecker delta functions.

Considering the vector spheroidal wave functions in the spheroidal coordinates, whose explicit expressions are the same as the ones used in Refs. [14, 25], the relationship between the vector spherical wave functions and vector spheroidal wave functions is given as:

$$(\mathbf{m},\mathbf{n})^{r(1)}_{\substack{e\\o}mn}(kR,\theta,\varphi) = \sum_{l=m,m+1}^{\infty}{}' \frac{2(n+m)!}{(2n+1)(n-m)!} \cdot \frac{i^{l-n}}{N_{ml}} d^{ml}_{n-m}(c)(\mathbf{M},\mathbf{N})^{r(1)}_{\substack{e\\o}ml}(c,\zeta,\eta,\varphi). \tag{15}$$

From Eq. (15), we can obtain the expansion of Gaussian beam in spheroidal coordinates. Accordingly, the electric component of the internal field and the scattered field can be expanded in terms of vector spheroidal wave functions. The unknown scattered coefficients can be determined by applying the boundary conditions of continuity of the tangential electromagnetic fields over the surface of the particle. Thus, the solution of scattering for Gaussian beam by a spheroidal particle can be obtained.

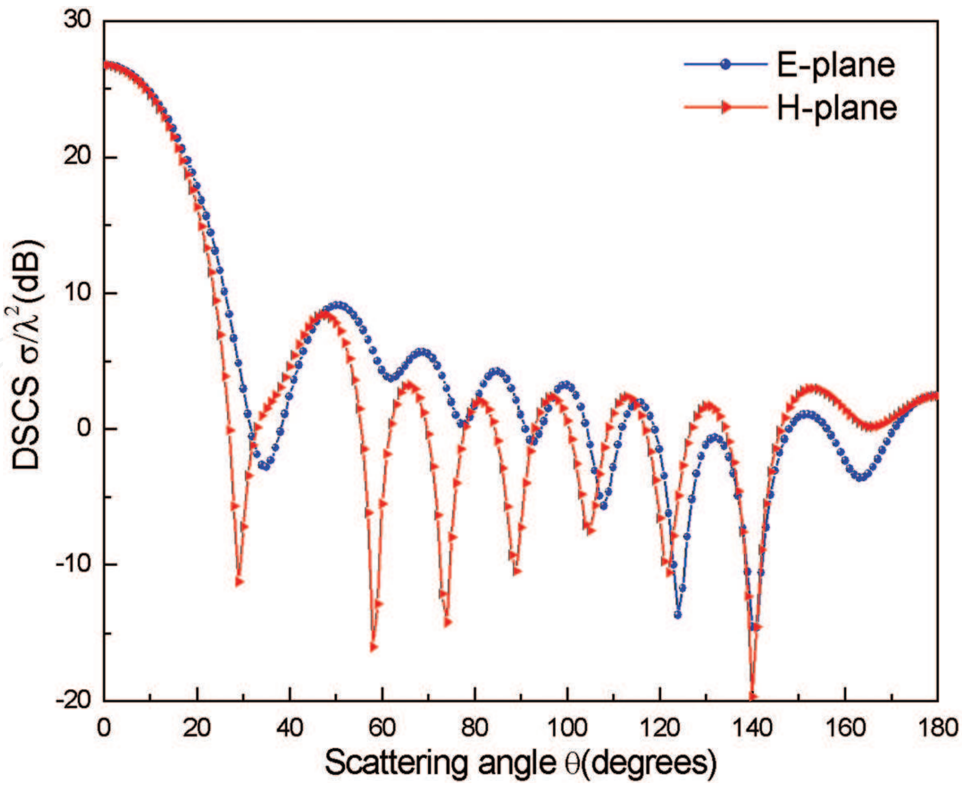

Figure 4. DSCS for incidence of a Gaussian beam on a dielectric spheroidal particle.

For the purpose of demonstration, **Figure 4** shows angular distributions of the DSCS for a spheroid with a semimajor axis and a semiminor axis being $a = 2.0\lambda$ and $b = 1.0\lambda$, respectively, and refractive index $m = 1.55$. The beam center is located at the origin of the particle system with beam waist radius of $\omega_0 = 2\lambda$, and the angle set of the beam is $\alpha = \beta = \gamma = 0^o$.

2.3. Light scattering by a circular cylindrical particle

The geometry of shaped beam scattering by a circular cylinder is illustrated in **Figure 5**. Similarly to a spheroidal particle, due to the lack of spherical symmetry, the arbitrary orientation is also compulsory in the case of GLMTs for cylinders. The expansion of the case of an arbitrary-shaped beam propagating in an arbitrary direction, based on which an approach to expand the shaped beam in terms of cylindrical vector wave functions natural to an infinite cylinder of arbitrary orientation is given below.

The vector cylindrical wave functions in the cylindrical coordinates (r, ϕ, z) are defined as

$$\begin{aligned} \mathbf{m}_{n\lambda}^{(j)}(kr, \phi, z) &= e^{ihz} e^{im\phi} [i \frac{m}{r} J_m(\lambda r) \mathbf{i}_r - \frac{\partial}{\partial r} J_m(\lambda r) \mathbf{i}_\varphi] \\ \mathbf{n}_{n\lambda}(kr, \phi, z) &= e^{ik_z z} e^{im\phi} \left[\frac{ih}{k} \frac{\partial}{\partial r} J_m(\lambda r) \mathbf{i}_r - \frac{hm}{kr} J_m(\lambda r) \mathbf{i}_\varphi + \frac{\lambda^2}{k} J_m(\lambda r) \mathbf{i}_z \right] \end{aligned} \tag{16}$$

where $(\mathbf{m}_{n\lambda}^{(j)}, \mathbf{n}_{n\lambda}^{(j)}) = (\mathbf{m}_{en\lambda}^{(j)}, \mathbf{n}_{en\lambda}^{(j)}) + i(\mathbf{m}_{on\lambda}^{(j)}, \mathbf{n}_{on\lambda}^{(j)})$ are the cylindrical vector wave functions of the first kind in the cylindrical coordinates (r, ϕ, z), and $(\mathbf{m}_{en\lambda}^{(j)}, \mathbf{n}_{en\lambda}^{(j)}), (\mathbf{m}_{on\lambda}^{(j)}, \mathbf{n}_{on\lambda}^{(j)})$ are the same as $(\mathbf{m}_{en\lambda}^{(j)}, \mathbf{n}_{en\lambda}^{(j)})e^{ihz}, (\mathbf{m}_{on\lambda}^{(j)}, \mathbf{n}_{on\lambda}^{(j)})e^{ihz}$ in defined by Stratton. The subscript "e" refers to even ϕ dependence while "o" refers to odd ϕ dependence, and we have $\lambda^2 + h^2 = k^2$, $h = k\cos\zeta$, $\lambda = k\sin\zeta$.

The relationship between the vector spherical wave functions and the vector cylindrical wave functions is defined as

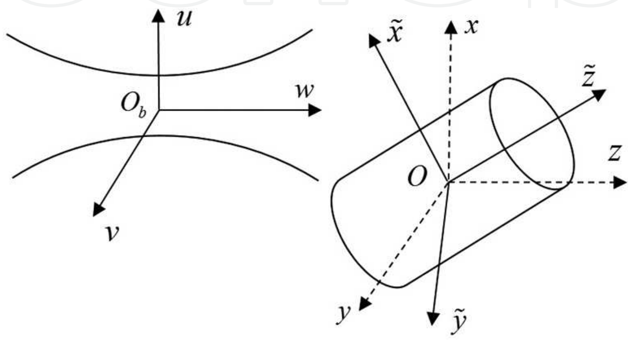

Figure 5. Geometry of a circular cylinder illuminated by a shaped beam.

$$\begin{aligned}\mathbf{m}_{mn}^{r(1)}(kR,\theta,\varphi) &= \int_0^{\pi}\left[c_{mn}(\zeta)\mathbf{m}_{m\lambda}^{(1)} + a_{mn}(\zeta)\mathbf{n}_{m\lambda}^{(1)}\right]e^{ihz}\sin\zeta d\zeta \\ \mathbf{n}_{mn}^{r(1)}(kR,\theta,\varphi) &= \int_0^{\pi}\left[c_{mn}(\zeta)\mathbf{n}_{m\lambda}^{(1)} + a_{mn}(\zeta)\mathbf{m}_{m\lambda}^{(1)}\right]e^{ihz}\sin\zeta d\zeta\end{aligned} \tag{17}$$

where

$$c_{mn}(\zeta) = \frac{i^{m-n+1}}{2k}\frac{dP_n^m(\cos\zeta)}{d(\cos\zeta)}, a_{mn}(\zeta) = \frac{mk}{\lambda^2}\frac{i^{m-n-1}}{2}P_n^m(\cos\zeta) \tag{18}$$

Based on Eqs. (17) and (1), we can obtain the expansion of the incident shaped beam in terms of the cylindrical vector wave functions in cylindrical coordinates as

$$\mathbf{E}^i = E_0\sum_{m=-\infty}^{\infty}\int_0^{\pi}[I_{m,TE}(\zeta)\mathbf{m}_{n\lambda} + I_{m,TM}(\zeta)\mathbf{n}_{n\lambda}]\sin\zeta d\zeta \tag{19}$$

where $I_{m,TE}(\zeta)$ and $I_{m,TM}(\zeta)$ are the BSCs in cylindrical coordinates, with explicit expressions

$$\begin{aligned}I_{m,TE}(\zeta) &= \sum_{n=|m|}^{\infty}[ig_{n,TE}^m c_{mn}(\zeta) + g_{n,TM}^m a_{mn}(\zeta)]. \\ I_{m,TM}(\zeta) &= \sum_{n=|m|}^{\infty}[ig_{n,TE}^m a_{mn}(\zeta) + g_{n,TM}^m c_{mn}(\zeta)]\end{aligned} \tag{20}$$

Accordingly, the electric component of the internal field and the scattered field can be expanded in terms of cylindrical vector wave functions. The unknown scattered coefficients can be determined by applying the boundary conditions of continuity of the tangential electromagnetic fields over the surface of the particle. Thus, the solution of scattering for Gaussian beam by a cylindrical particle can be obtained.

3. Light scattering by complex particles of arbitrary shapes and structure

3.1. Surface integral equation method

Many particles encountered in nature or produced in industrial processes, such as raindrops, ice crystals, biological cells, dust grains, daily cosmetics, and aerosols in the atmosphere, not only have irregular shapes but also have complex structures. The study of light scattering by these complex particles is essential in a wide range of scientific fields with many practical applications, including optical manipulation, particle detection and discrimination, design of new optics devices, etc. Here, we introduce the surface integral equation method (SIEM) [26–28] to simulate the light scattering by arbitrarily shaped particles with multiple internal dielectric inclusions of arbitrary shape, which can be reduced to the case of arbitrarily shaped homogeneous dielectric particles. For SIEM, the incident Gaussian beam can be described

http://dx.doi.org/10.5772/66662

using the method of combing Davis-Barton fifth-order approximation [29] in combination with rotation Euler angles [30].

Now, let us consider the problem of Gaussian beam scattering by an arbitrarily shaped particle with multiple dielectric inclusions of arbitrary shape. As illustrated in **Figure 6**, let S_h represent the surface of the host particle and S_i represent the surface of the $ith(i = 1, 2, \cdots, N)$ inclusion, with N being the total number of the internal inclusions. Let ε_h, μ_h and ε_i, μ_i represent the permittivity and permeability of the host particle and the *ith* dielectric inclusion, respectively. The surrounding medium is also considered to be free space with parameters ε_0 and μ_0. Let Ω_0, Ω_i and Ω_h, respectively, denote the free space region, the region occupied by the *ith* internal inclusion and the region occupied by the host particle except those occupied by all the inclusions. Introducing equivalent electromagnetic currents $\mathbf{J}_h$, M_h on S_h and $\mathbf{J}_i$, M_i on $S_i(i = 1, 2, \cdots, N)$. On the bases of the surface equivalence principle, the fields in each region can be expressed in terms of the equivalent electric and magnetic currents. Specifically, the scattered fields $\mathbf{E}_0^{sca}$ and $\mathbf{H}_0^{sca}$ in the region Ω_0, due to the equivalent electromagnetic currents $\mathbf{J}_h$ and M_h on S_h, can be expressed as Eqs. (21) and (22)

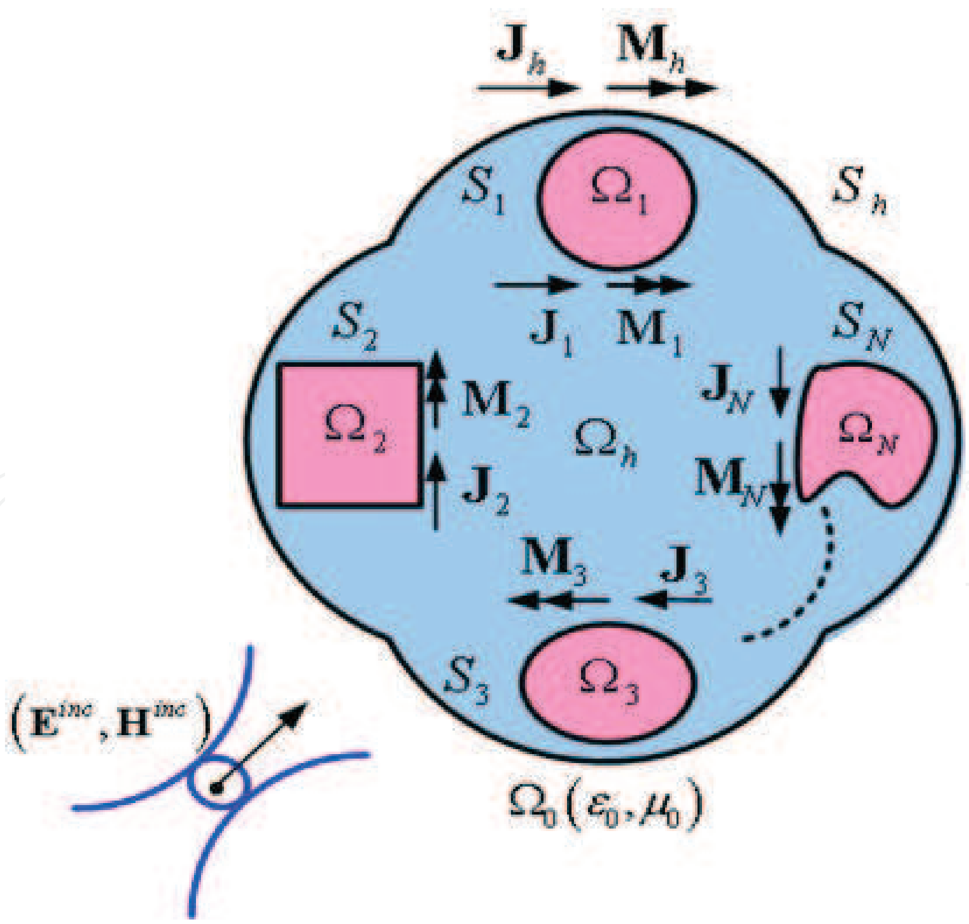

Figure 6. Configuration of an arbitrarily shaped particle with multiple internal inclusions of arbitrary shape.

$$\mathbf{E}_0^{sca} = Z_0 \mathbf{L}_0^{S_h}(\mathbf{J}_h) - \mathbf{K}_0^{S_h}(\mathbf{M}_h) \tag{21}$$

$$\mathbf{H}_0^{sca} = \mathbf{K}_0^{S_h}(\mathbf{J}_h) + \frac{1}{Z_0}\mathbf{L}_0^{S_h}(\mathbf{M}_h) \tag{22}$$

where the integral operators $\mathbf{L}_0^S$ and $\mathbf{K}_0^S$ are defined as

$$\mathbf{L}_0^S(\mathbf{X}) = -ik_0 \iint_S \left[\mathbf{X}(\mathbf{r}') + \frac{1}{k_0^2}\nabla\nabla' \cdot \mathbf{X}(\mathbf{r}')\right] G_0(\mathbf{r}, \mathbf{r}') dS' \tag{23}$$

$$\mathbf{K}_0^S(\mathbf{X}) = -\iint_S \mathbf{X}(\mathbf{r}') \times G_0(\mathbf{r}, \mathbf{r}') dS' \tag{24}$$

in which the subscript "0" represents the medium in which the scattered fields are computed and the superscript "S" represents the surface on which the integration is performed, $G_0(\mathbf{r}, \mathbf{r}')$ is the Green's function in region Ω_0. The fields in region Ω_h are produced by the equivalent electromagnetic currents $-\mathbf{J}_h$, $-M_h$ on S_h and $\mathbf{J}_i$, M_i on $S_i (i = 1, 2, \ldots, N)$ and can be expressed as

$$\mathbf{E}_h = \left[Z_h \mathbf{L}_h^{S_h}(-\mathbf{J}_h) - \mathbf{K}_h^{S_h}(-\mathbf{M}_h)\right] + \sum_{i=1}^{N}\left[Z_h \mathbf{L}_h^{S_i}(\mathbf{J}_i) - \mathbf{K}_h^{S_i}(\mathbf{M}_i)\right] \tag{25}$$

$$\mathbf{H}_h = \left[\mathbf{K}_h^{S_h}(-\mathbf{J}_h) + \frac{1}{Z_h}\mathbf{L}_h^{S_h}(-\mathbf{M}_h)\right] + \sum_{i=1}^{N}\left[\mathbf{K}_h^{S_i}(\mathbf{J}_i) + \frac{1}{Z_h}\mathbf{L}_h^{S_i}(\mathbf{M}_i)\right]. \tag{26}$$

Also based on the surface equivalence principle, the fields $\mathbf{E}_i$ and $\mathbf{H}_i$ in region $\Omega_i (i = 1, 2, \cdots, N)$ can be expressed in terms of the equivalent electric and magnetic currents $-\mathbf{J}_i$ and $-M_i$ as

$$\mathbf{E}_i = Z_i \mathbf{L}_i^{S_i}(-\mathbf{J}_i) - \mathbf{K}_i^{S_i}(-\mathbf{M}_i) \tag{27}$$

$$\mathbf{H}_i = \mathbf{K}_i^{S_i}(-\mathbf{J}_i) + \frac{1}{Z_i}\mathbf{L}_i^{S_i}(-\mathbf{M}_i) \tag{28}$$

where $Z_i = \sqrt{\mu_i/\varepsilon_i}$ and the operators $\mathbf{L}_i^S$ and $\mathbf{K}_i^S$ are also defined similarly to $\mathbf{L}_0^S$ and $\mathbf{K}_0^S$, provided that all the subscripts are changed from "0" to "i".

By enforcing the continuity of the tangential electromagnetic fields across each surface, the following integral equations may be established

$$\begin{aligned}&|Z_0\mathbf{L}_0^{S_h}(\mathbf{J}_h)-\mathbf{K}_0^{S_h}(\mathbf{M}_h)+Z_h\mathbf{L}_h^{S_h}(\mathbf{J}_h)-\mathbf{K}_h^{S_h}(\mathbf{M}_h)\\&-\sum_{i=1}^{N}[Z_h\mathbf{L}_h^{S_i}(\mathbf{J}_i)-\mathbf{K}_h^{S_i}(\mathbf{M}_i)]=-\mathbf{E}^{inc}|_{\tan(S_h)}\end{aligned}\tag{29}$$

$$\begin{aligned}&|\mathbf{K}_0^{S_h}(\mathbf{J}_h)+\frac{1}{Z_0}\mathbf{L}_0^{S_h}(\mathbf{M}_h)+\mathbf{K}_h^{S_h}(\mathbf{J}_h)+\frac{1}{Z_h}\mathbf{L}_h^{S_h}(\mathbf{M}_h)\\&-\sum_{i=1}^{N}\left[\mathbf{K}_h^{S_i}(\mathbf{J}_i)+\frac{1}{Z_h}\mathbf{L}_h^{S_i}(\mathbf{M}_i)\right]=-\mathbf{H}^{inc}|_{\tan(S_h)}\end{aligned}\tag{30}$$

$$\begin{aligned}&|Z_h\mathbf{L}_h^{S_h}(\mathbf{J}_h)-\mathbf{K}_h^{S_h}(\mathbf{M}_h)-Z_i\mathbf{L}_i^{S_i}(\mathbf{J}_i)+\mathbf{K}_i^{S_i}(\mathbf{M}_i)-Z_h\mathbf{L}_h^{S_i}(\mathbf{J}_i)\\&+\mathbf{K}_h^{S_i}(\mathbf{M}_i)-\sum_{j=1,j\neq i}^{N}[Z_h\mathbf{L}_h^{S_j}(\mathbf{J}_j)-\mathbf{K}_h^{S_j}(\mathbf{M}_j)]=0|_{\tan(S_i)}\end{aligned}\tag{31}$$

$$\begin{aligned}&|\mathbf{K}_h^{S_h}(\mathbf{J}_h)+\frac{1}{Z_h}\mathbf{L}_h^{S_h}(\mathbf{M}_h)-\mathbf{K}_i^{S_i}(\mathbf{J}_i)-\frac{1}{Z_i}\mathbf{L}_i^{S_i}(\mathbf{M}_i)-\mathbf{K}_h^{S_i}(\mathbf{J}_i)\\&-\frac{1}{Z_h}\mathbf{L}_h^{S_i}(\mathbf{M}_i)-\sum_{j=1,j\neq i}^{N}\left[\mathbf{K}_h^{S_j}(\mathbf{J}_j)+\frac{1}{Z_h}\mathbf{L}_h^{S_j}(\mathbf{M}_j)\right]=0|_{\tan(S_i)}\end{aligned}\tag{32}$$

where the subscripts " $\tan(S_p)$" and " $\tan(S_i)$" stand for tangential components of the fields on S_h and $S_i(i=1,2,\cdots,N)$, respectively. Applying the method of moments (MOMs) with RWG basis functions to the above established integral equations yields a linear system of equations as follows:

$$\begin{bmatrix} Z_{J_hJ_h} & Z_{J_hM_h} & Z_{J_hJ_1} & \cdots & Z_{J_hJ_N} & Z_{J_hM_1} & \cdots & Z_{J_hM_N}\\ Z_{M_hJ_h} & Z_{M_hM_h} & Z_{M_hJ_1} & \cdots & Z_{M_hJ_N} & Z_{M_hM_1} & \cdots & Z_{M_hM_N}\\ Z_{J_1J_h} & Z_{J_1M_h} & Z_{J_1J_1} & \cdots & Z_{J_1J_N} & Z_{J_1M_1} & \cdots & Z_{J_1M_N}\\ \vdots & \vdots & \vdots & \vdots & \vdots & \vdots & \vdots & \vdots\\ Z_{J_NJ_h} & Z_{J_NM_h} & Z_{J_NJ_1} & \cdots & Z_{J_NJ_N} & Z_{J_NM_1} & \cdots & Z_{J_NM_N}\\ Z_{M_1J_h} & Z_{M_1M_h} & Z_{M_1J_1} & \cdots & Z_{M_1J_N} & Z_{M_1M_1} & \cdots & Z_{M_1M_N}\\ \vdots & \vdots & \vdots & \vdots & \vdots & \vdots & \vdots & \vdots\\ Z_{M_NJ_h} & Z_{M_NM_h} & Z_{M_NJ_1} & \cdots & Z_{M_NJ_N} & Z_{M_NM_1} & \cdots & Z_{M_NM_N}\end{bmatrix}\begin{Bmatrix} J_h\\ M_h\\ J_1\\ \vdots\\ J_N\\ M_1\\ \vdots\\ M_N\end{Bmatrix}=\begin{Bmatrix} b_E\\ b_H\\ 0\\ \vdots\\ 0\\ 0\\ \vdots\\ 0\end{Bmatrix}.\tag{33}$$

The resultant matrix Eq. (33) can also be solved iteratively by employing the multilevel fast multipole algorithm (MLFMA). Once obtained the unknown equivalent electromagnetic currents, the far-zone scattered fields and DSCS can be calculated.

3.2. Numerical results

First, we consider the reduced case of arbitrarily shaped homogeneous dielectric particles. To illustrate the validity of the proposed method, the scattering of a focused Gaussian beam by a homogeneous spherical dielectric particle is considered. The radius of the spherical particle is $r = 1.0\lambda$, and the refractive index of the particle is $m = 2.0$. The beam center is located at the origin of the particle system with beam waist radius of $\omega_0 = 2\lambda$, and the angle set of the beam is $\alpha = \beta = \gamma = 0^o$. **Figure 7** shows the computed DSCS as a function of the scattering angle in the E-plane. For comparison, the results obtained using the GLMT are given in the same figure. Excellent agreements are observed between them.

To illustrate the validity of the proposed method for composite particles with inclusions, we consider the scattering a Gaussian beam by a spheroidal particle with a spherical inclusion at the center, as shown in **Figure 8**. The semimajor axis and the semiminor axis of the host spheroid are $a = 2.0\lambda$ and $b = 1.0\lambda$, respectively. The radius of the spherical inclusion is $r_i = 0.5\lambda$. The host spheroid is characterized by refractive index $m = 2.0$. For the case of dielectric inclusion, the refractive index is $m_1 = 1.414$. The particle is illuminated by an on-axis normally incident Gaussian beam with $\omega_0 = 2.0\lambda$ and $x_0 = y_0 = z_0 = 0.0$. The computed DSCSs as a function of the scattering angle in the E-plane and the H-plane are shown in **Figure 9**. For comparison, the result obtained using the analytical theory GLMT is given in the same figure. Excellent agreements are observed between them.

Finally, the scattering of an obliquely incident Gaussian beam by a cubic particle containing 27 randomly distributed spherical inclusions is considered to illustrate the capabilities of the proposed method. The center of the host cube is located at the origin of the particle system and the side length of the cube is $l = 3.0\lambda$. All the spherical inclusions are assumed to be uniform, and the positions are generated using the Monte Carlo method described in Ref. [31] with fractional volume $f = 6.0\%$, as shown in **Figure 10**. The host cube is characterized by

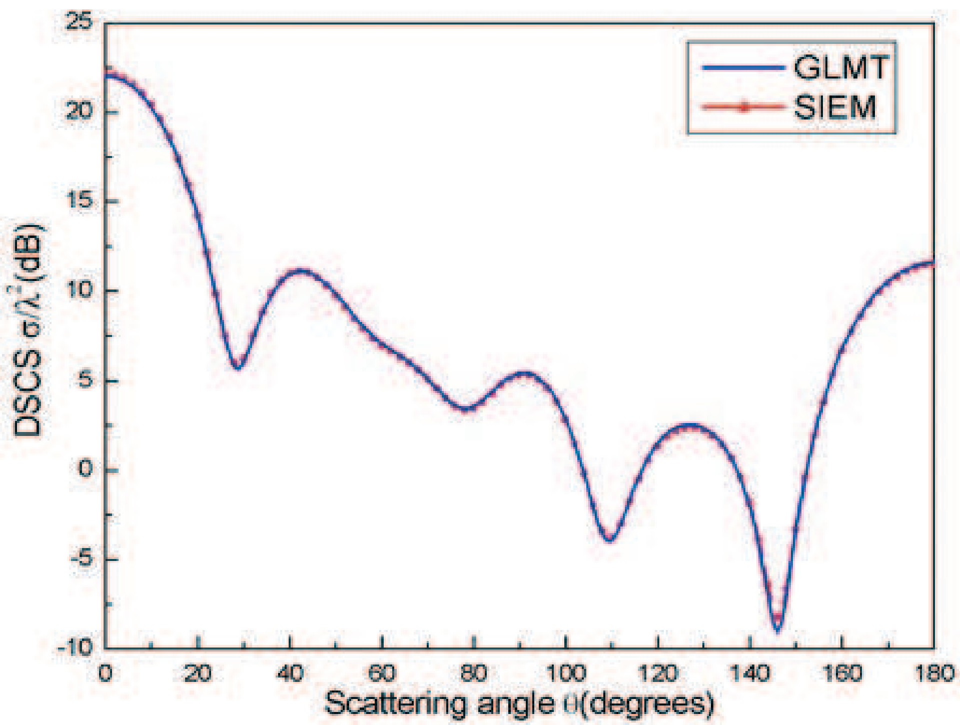

Figure 7. Comparison of the DSCS for a spherical dielectric particle obtained from the SIEM and the GLMT.

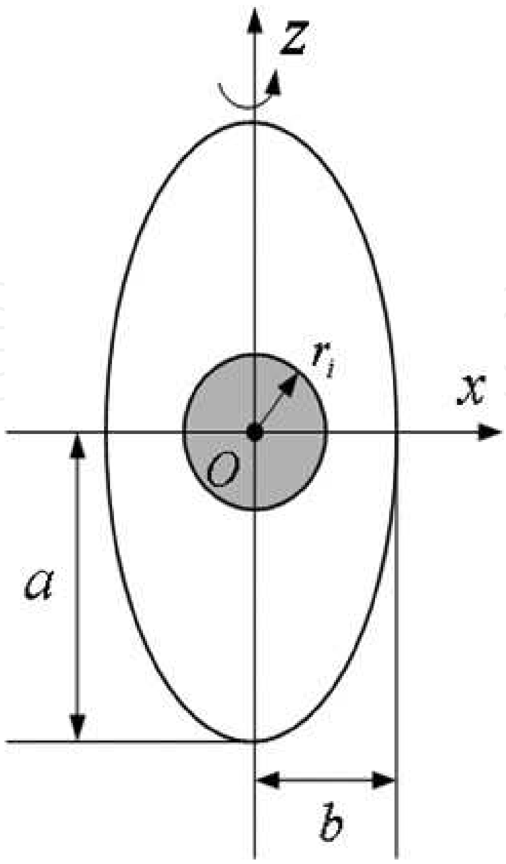

Figure 8. Geometry of a spheroidal particle with a spherical inclusion at the center.

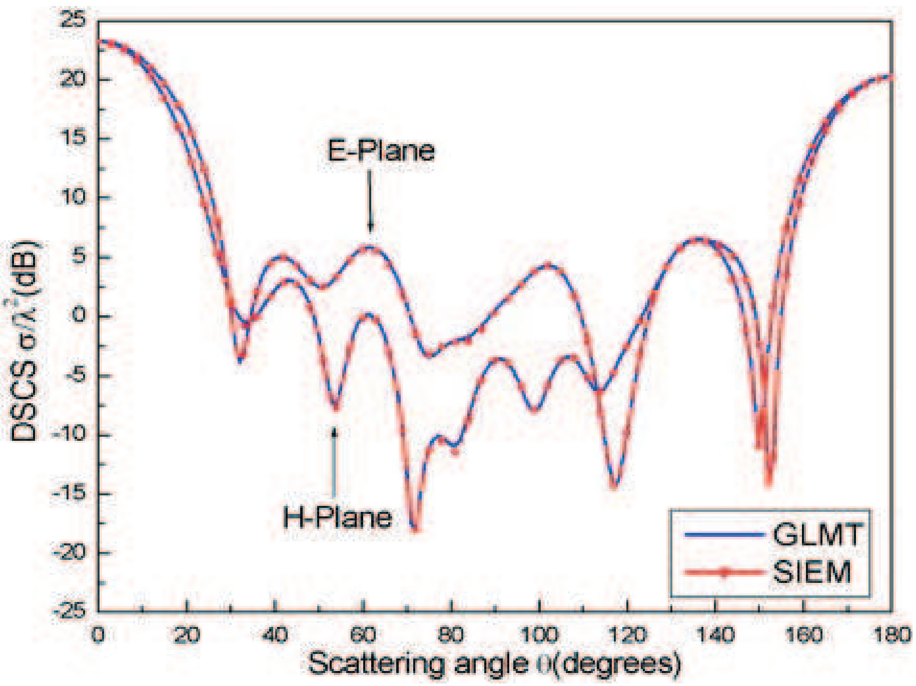

Figure 9. Comparison of the DSCSs for a spheroidal particle with a spherical inclusion at the center obtained from the SIEM and that from the GLMT.

refractive index $m = 1.2–i0.2$. For the case of dielectric inclusion, the complex refractive index is $m = 1.5–i0.1$. The beam waist is centered at $x_0 = y_0 = z_0 = 0.0$ with a beam waist radius of $\omega_0 = 2.0\lambda$. The rotation Euler angles are $\alpha = 0^o, \beta = 45^o$ and $\gamma = 0^o$. **Figure 11** presents the simulated DSCSs as a function of the scattering angle in both the E-plane and the H-plane.

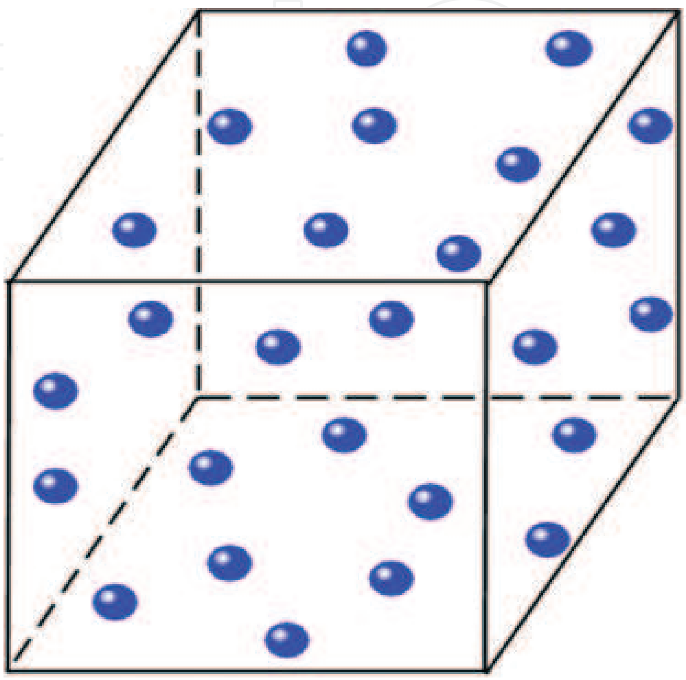

Figure 10. Illustration of a cubic particle containing 27 randomly distributed spherical inclusions.

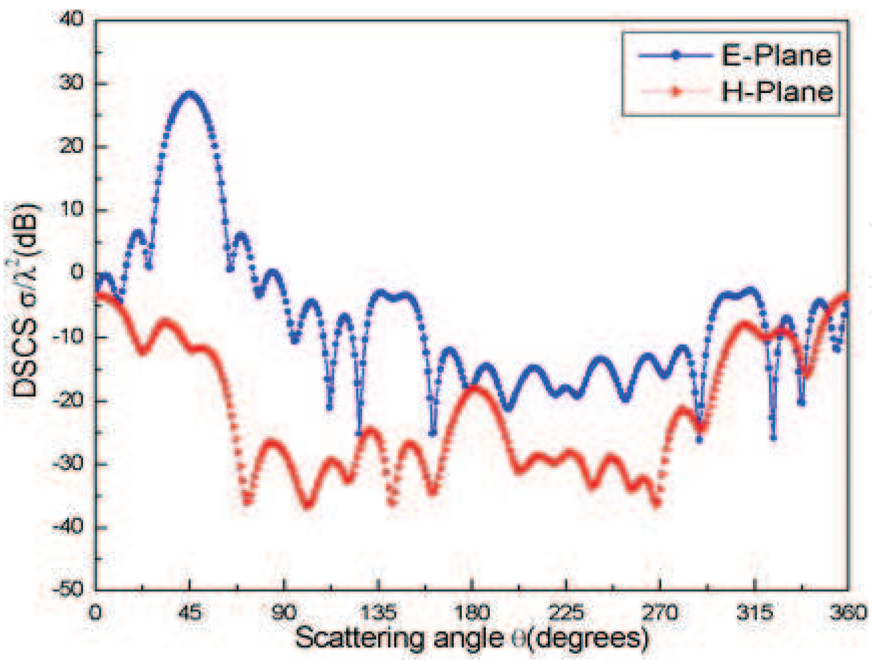

Figure 11. The DSCSs for a cubic particle with 27 randomly distributed spherical inclusions.

4. Light scattering by random discrete particles

Due to the wide range of possible applications in academic research and industry, the problem of light scattering by random media composed of many discrete particles is a subject of broad interest. Over the past few decades, some theories and numerical methods have been developed to study the light scattering by random discrete particles [32–48]. In this section, we introduce a hybrid finite element-boundary integral-characteristic basis function method (FE-BI-CBFM) to simulate the light scattering by random discrete particles [49]. In this hybrid technique, the finite element method (FEM) is used to obtain the solution of the vector wave equation inside each particle and the boundary integral equation (BIE) is applied on the surfaces of all the particles as a global boundary condition. To reduce computational burdens, the characteristic basis function method (CBFM) is introduced to solve the resultant FE-BI matrix equation. The incident light is assumed to be Gaussian laser beam.

4.1. FE-BI-CBFM for random discrete particles

Now, let us consider the scattering of an arbitrarily incident focused Gaussian beam by multiple discrete particles with a random distribution, as depicted in **Figure 12**. For simplicity, the background region, which is considered to be free space, is denoted as Ω_0, the region

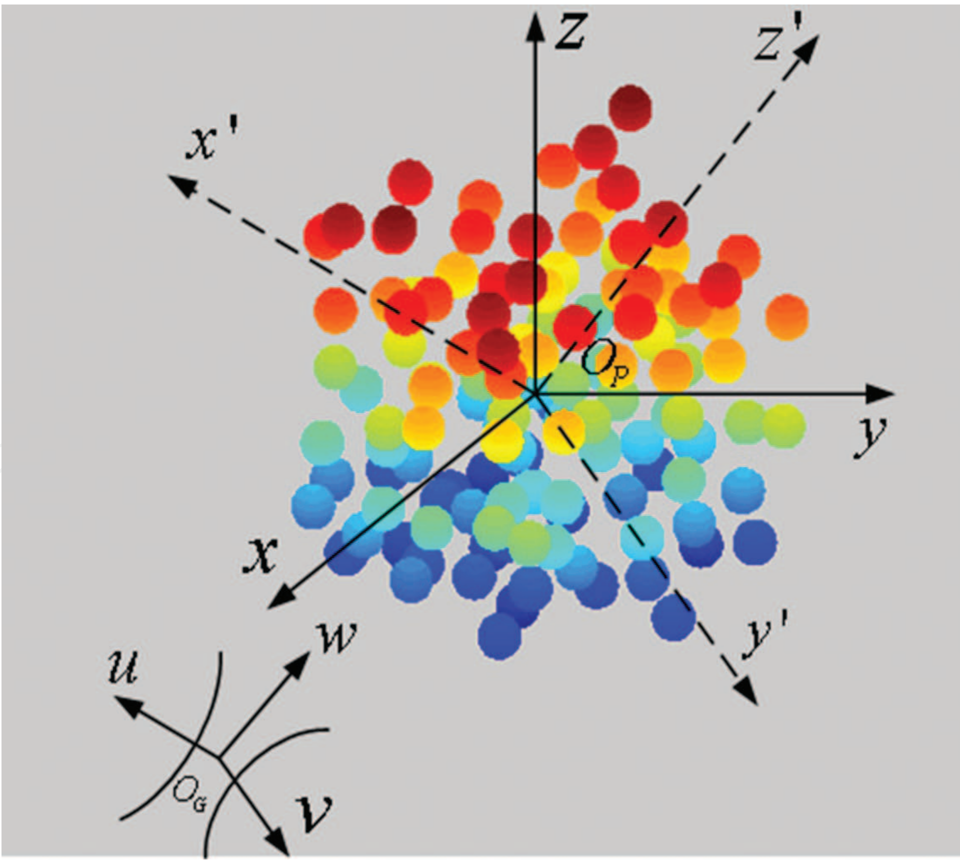

Figure 12. Illustration of an arbitrarily incident Gaussian beam impinges on multiple discrete particles with a random distribution.

occupied by the *ith* particle is denoted as $\Omega_i (i = 1, 2, \ldots, M)$, and the corresponding volume and boundary surface are denoted as V_i and S_i, respectively. In accordance with the variational principle [50], the solution to the field in region Ω_i can be obtained by solving an equivalent variational problem with the functional given by

$$F(\mathbf{E}_i) = \frac{1}{2}\iiint_{V_i}\left[\frac{1}{\mu_r}(\nabla\times\mathbf{E}_i)\cdot(\nabla\times\mathbf{E}_i) - k_0^2\varepsilon_r\mathbf{E}_i\cdot\mathbf{E}_i\right]dV + ik_0 Z_0\iint_{S_i}(\mathbf{E}_i\times\mathbf{H}_i)\cdot\widehat{n}_i dS. \tag{34}$$

where $\hat{n}_i$ denotes the outward unit vector normal to S_i, ε_r, and μ_r are the relative permittivity and permeability of the particles. Using the FEM with Whitney vector basis functions defined on tetrahedral elements [50], the functional F can be converted into a sparse matrix equation

$$\begin{bmatrix} K_i^{II} & K_i^{IS} & 0 \\ K_i^{SI} & K_i^{SS} & B_i \end{bmatrix}\begin{Bmatrix} E_i^I \\ E_i^S \\ H_i^S \end{Bmatrix} = \begin{Bmatrix} 0 \\ 0 \end{Bmatrix} \tag{35}$$

where $[K_i^{II}]$, $[K_i^{IS}]$, $[K_i^{SI}]$ and $[K_i^{SS}]$ are contributed by the volume integral in Eq. (34), whereas $[B_i]$ is contributed by the surface integral. Also, $\{E_i^I\}$ is a vector containing the discrete electric fields inside V_i, and $\{E_i^S\}$ and $\{H_i^S\}$ are the vectors containing the discrete electric and magnetic fields on S_i, respectively.

Since Eq. (35) is independent of the excitation, we can remove the interior unknowns to derive a matrix equation that only includes the unknowns on S_i, as follows:

$$\left[\tilde{K}_i^{SS}\right]\left\{E_i^S\right\} + [B_i]\left\{H_i^S\right\} = \{0\} \tag{36}$$

where

$$\left[\tilde{K}_i^{SS}\right] = \left[K_i^{SS}\right] - \left[K_i^{SI}\right]\left[K_i^{II}\right]^{-1}\left[K_i^{IS}\right]. \tag{37}$$

For the convenience of description, we write the relation between $\left\{E_i^S\right\}$ and $\left\{H_i^S\right\}$ as

$$\left\{E_i^S\right\} = [S_i]\left\{H_i^S\right\} \tag{38}$$

where

$$[S_i] = -\left[\tilde{K}_i^{SS}\right]^{-1}[B_i]. \tag{39}$$

It is worth to notice that the calculations of Eqs. (37) and (39) in each particle are independent and can be completely parallelized. Furthermore, since the particles are uniform, the coefficient matrices are the same for each particle. This implies that only one particle needs to be dealt with to obtain all the matrices $[S_i], (i = 1, 2, \ldots, M)$. For simplicity, let $[S_1] = [S_2] = \cdots [S_M] = [S]$. As a result, the relation between the electric and magnetic fields on all the surfaces can be written as

$$\begin{Bmatrix} E_1^S \\ E_2^S \\ \vdots \\ E_M^S \end{Bmatrix} = \begin{bmatrix} S & & & \\ & S & & \\ & & \ddots & \\ & & & S \end{bmatrix} \begin{Bmatrix} H_1^S \\ H_2^S \\ \\ H_M^S \end{Bmatrix}. \tag{40}$$

To formulate the field in region Ω_0, we introduce the equivalent electric and magnetic currents $\mathbf{J}_i$ and M_i on $S_i(i = 1, 2, \ldots, M)$. By invoking Huygens's principle, the scattered fields in region Ω_0, due to the equivalent currents $\mathbf{J}_i$ and M_i on $S_i(i = 1, 2, \ldots, M)$, can be represented as

$$\mathbf{E}_0^{sca} = \sum_{i=1}^{M} [Z_0 \mathbf{L}_i(\mathbf{J}_i) - \mathbf{K}_i(\mathbf{M}_i)] \tag{41}$$

$$\mathbf{H}_0^{sca} = \sum_{i=1}^{M} \left[\frac{1}{Z_0} \mathbf{L}_i(\mathbf{M}_i) + \mathbf{K}_i(\mathbf{J}_i) \right]. \tag{42}$$

Enforcing boundary condition on S_i yields an electric field integral equation (EFIE)

$$\left| -\widehat{n}_i \times \mathbf{M}_i + \sum_{j=1}^{M} [Z_0 \mathbf{L}_j(\mathbf{J}_j) - \mathbf{K}_j(\mathbf{M}_j)] = -\mathbf{E}^{inc} \right|_{\tan(S_i)} \tag{43}$$

and a magnetic field integral equation (MFIE)

$$\left| -\mathbf{J}_i \times \widehat{n}_i + \sum_{j=1}^{M} \left[\frac{1}{Z_0} \mathbf{L}_j(\mathbf{M}_j) + \mathbf{K}_j(J_j) \right] = -\mathbf{H}^{inc} \right|_{\tan(S_i)} \tag{44}$$

where the subscript " $\tan(S_i)$" stands for tangential components of the fields on S_i. To remove the interior resonance, we employ the CFIE, which combines the EFIE and MFIE in the following form

$$\mathrm{CFIE}_i = \mathrm{EFIE}_i + \widehat{n}_i \times Z_0 \mathrm{MFIE}_i \tag{45}$$

where the subscript i denotes the integral equation is established by enforcing boundary condition on S_i. Using the MOM with RWG vector basis functions, which are completely compatible with the Whitney vector basis functions [50], the CFIE can be converted into a full matrix equation

$$\begin{bmatrix} P_{11} & P_{12} & \cdots & P_{1M} \\ P_{21} & P_{22} & \cdots & P_{2M} \\ \vdots & \vdots & \ddots & \vdots \\ P_{M1} & P_{M2} & \cdots & P_{MM} \end{bmatrix} \begin{Bmatrix} E_1^S \\ E_2^S \\ \vdots \\ E_M^S \end{Bmatrix} + \begin{bmatrix} Q_{11} & Q_{12} & \cdots & Q_{1M} \\ Q_{21} & Q_{22} & \cdots & Q_{2M} \\ \vdots & \vdots & \ddots & \vdots \\ Q_{M1} & Q_{M2} & \cdots & Q_{MM} \end{bmatrix} \begin{Bmatrix} H_1^S \\ H_2^S \\ \vdots \\ H_M^S \end{Bmatrix} = \begin{Bmatrix} b_1 \\ b_2 \\ \vdots \\ b_M \end{Bmatrix}. \tag{46}$$

The expressions of the elements for matrices $[P_{ij}]$ and $[Q_{ij}]$ and vectors $\{b_i\}, (i, j = 1, 2, \cdots, M)$ can be found in Ref. [49]. Substituting Eq. (40) into Eq. (46), we obtain the final FE-BI matrix equation

$$\left(\begin{bmatrix} P_{11} & P_{12} & \cdots & P_{1M} \\ P_{21} & P_{22} & \cdots & P_{2M} \\ \vdots & \vdots & \ddots & \vdots \\ P_{M1} & P_{M2} & \cdots & P_{MM} \end{bmatrix} \begin{bmatrix} S & & & \\ & S & & \\ & & \ddots & \\ & & & S \end{bmatrix} + \begin{bmatrix} Q_{11} & Q_{12} & \cdots & Q_{1M} \\ Q_{21} & Q_{22} & \cdots & Q_{2M} \\ \vdots & \vdots & \ddots & \vdots \\ Q_{M1} & Q_{M2} & \cdots & Q_{MM} \end{bmatrix} \right) \begin{Bmatrix} H_1^S \\ H_2^S \\ \vdots \\ H_M^S \end{Bmatrix} = \begin{Bmatrix} b_1 \\ b_2 \\ \vdots \\ b_M \end{Bmatrix}. \tag{47}$$

The above equation can be written in a more compact form as

$$\begin{bmatrix} \mathbf{Z}_{11} & \mathbf{Z}_{12} & \cdots & \mathbf{Z}_{1M} \\ \mathbf{Z}_{21} & \mathbf{Z}_{22} & \cdots & \mathbf{Z}_{2M} \\ \vdots & \vdots & \ddots & \vdots \\ \mathbf{Z}_{M1} & \mathbf{Z}_{M2} & \cdots & \mathbf{Z}_{MM} \end{bmatrix} \begin{bmatrix} \mathbf{J}_1 \\ \mathbf{J}_2 \\ \vdots \\ \mathbf{J}_M \end{bmatrix} = \begin{bmatrix} \mathbf{V}_1 \\ \mathbf{V}_2 \\ \vdots \\ \mathbf{V}_M \end{bmatrix} \tag{48}$$

where $\mathbf{Z}_{ij} = [P_{ij}][S] + [Q_{ij}]$ are $N \times N$ matrices, $\mathbf{J}_i = \{H_i^S\}$ and $\mathbf{V}_i = \{b_i\}(i, j = 1, 2, \cdots, M)$ are column vectors of length N, with N being the number of unknowns for magnetic field on the surface of each particle. The solution to Eq. (51) can be obtained by the CBFM described in Ref. [47]. It is based on the use of a set of high-level basis functions, called the characteristic basis functions (CBFs) that are constructed according to the Foldy-Lax multiple scattering equations. These CBFs are comprised of primary CBFs arising from the self-interactions from within the particles, and secondary CBFs that account for the mutual coupling effects from the rest of the particles. Based on the Foldy-Lax equations, the primary CBF for each particle is constructed by exciting that particular particle with the incident field and ignoring the scattered fields of all other particles. By replacing the incident field with the scattered fields, the first secondary CBF for a given particle can be constructed. This is because the primary CBFs induced on all particles except from itself. In this way, additional secondary CBFs can be constructed similarly. A significant reduction in the number of unknowns is realized due to the use of these basis functions, which gives a substantial size reduction in the resultant matrix. Consequently, it enables us to handle the reduced matrix using a direct solver instead of iteration method. Furthermore, the computational burden can be significantly relieved since this method only requires the solution of small-size matrix equations associated with isolated particles. The detailed description of CBFM can be found in Ref. [49].

4.2. Numerical results and discussion

In what follows, some numerical results are presented. First, we consider the scattering of Gaussian beam by 125 randomly distributed conducting spherical particles with a radius of

http://dx.doi.org/10.5772/66662

$r = 0.25\lambda$, as shown in **Figure 12**. The particle positions are generated randomly in a cubic box with which the fractional volume is 10%. The incident Gaussian beam center is centered at $x_0 = y_0 = z_0 = 0.0$, and the angle set of the beam is $\alpha = \beta = \gamma = 0^o$. Results of DSCS are displayed in **Figure 13** as a function of the scattering angle in the E-plane. As can be seen from the figure, the DSCS for Gaussian beams is smaller than that for a plane wave. In addition, for a Gaussian beam incidence with a relatively large waist radius of $\omega_0 = 20\lambda$, the results are in excellent agreement with the results in the case of plane wave illumination.

We then consider the multiple scattering of an obliquely incident Gaussian beam by 512 randomly distributed inhomogeneous spherical particles with which the fractional volume is 10%. Each primary particle consists of a conducting sphere with radius $r = 0.1\lambda$ covered by a dielectric coating with a thickness $t = 0.1\lambda$. The complex refractive index of the coating layer is $m = 1.6–i0.2$. The beam waist is centered at $(x_0, y_0, z_0) = (-1.0, -1.0, -1.0)\lambda$ with a beam waist radius of $\omega_0 = 2.5\lambda$, and the rotation Euler angles are specified as $\alpha = 45, \beta = 45$ and $\gamma = 0$. **Figure 14** presents the simulated DSCSs as a function of the scattering angle.

Finally, we use the present numerical method to simulate the multiple scattering of Gaussian beam by 1000 randomly distributed homogeneous dielectric spherical particles with which the fractional volume is 10%. The radius and the refractive index of the primary particles are assumed as $r = 50$ nm and $m = 1.6–i0.6$, respectively. The wavelength of the incident Gaussian beam is assumed to be $\lambda = 532$ nm. The location of the beam waist center is $x_0 = y_0 = z_0 = 0.0$, and the beam waist radius equals to $\omega_0 = 2.0\lambda$. The Euler angles are $\alpha = 45, \beta = 45$ and $\gamma = 0$. The DSCS is displayed in **Figure 15**. Furthermore, the DSCS of the ensembles of randomly distributed particles for the independent scattering is also calculated. Specifically, an

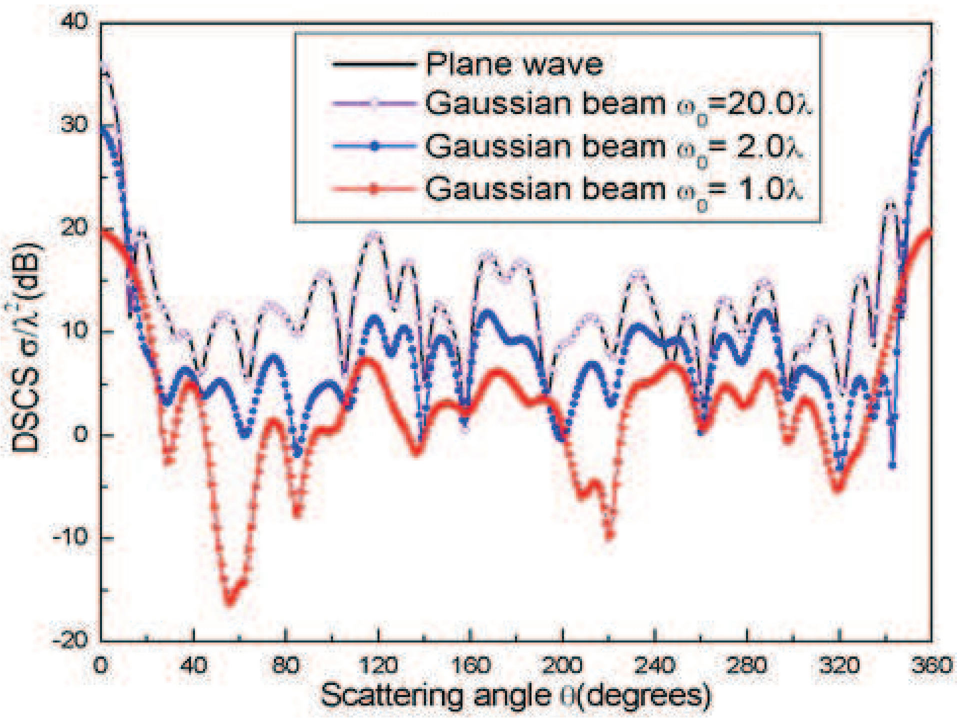

Figure 13. DSCS for 125 randomly distributed conducting spherical particles.

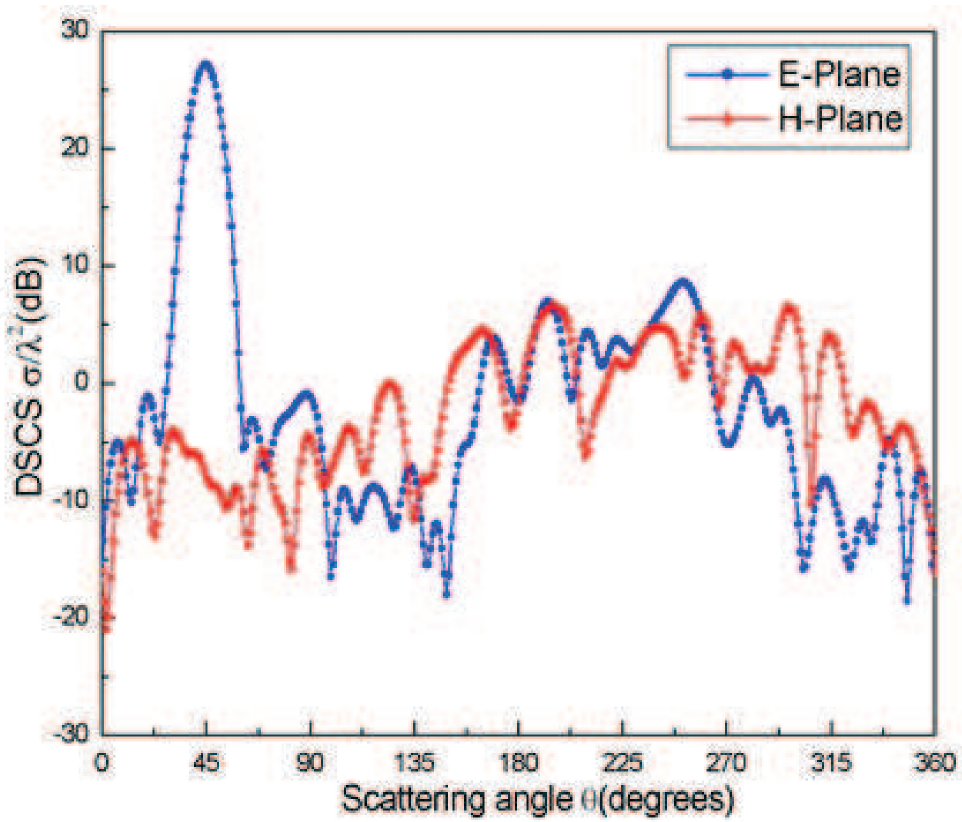

Figure 14. DSCS for 512 randomly distributed inhomogeneous spherical particles.

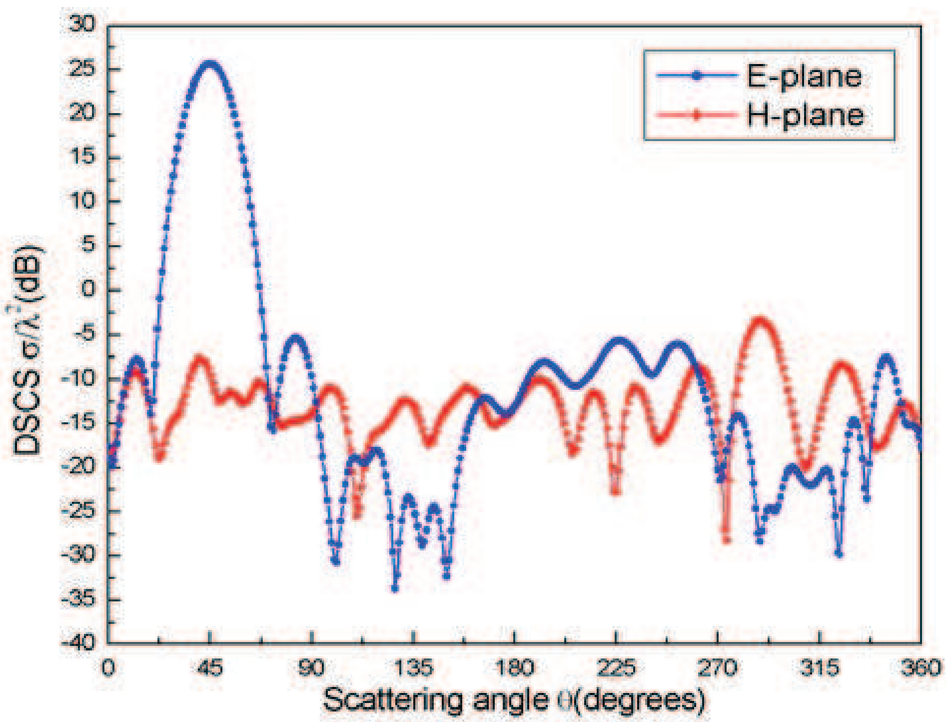

Figure 15. DSCS for 1000 randomly distributed homogeneous dielectric spherical particles.

individual particle is assumed to scatter light without interactions with other particle in the ensemble. The computed DSCS for the independent scattering is displayed in **Figures 16** and **17**. Comparisons between independent scattering and the multiple scattering are made. The

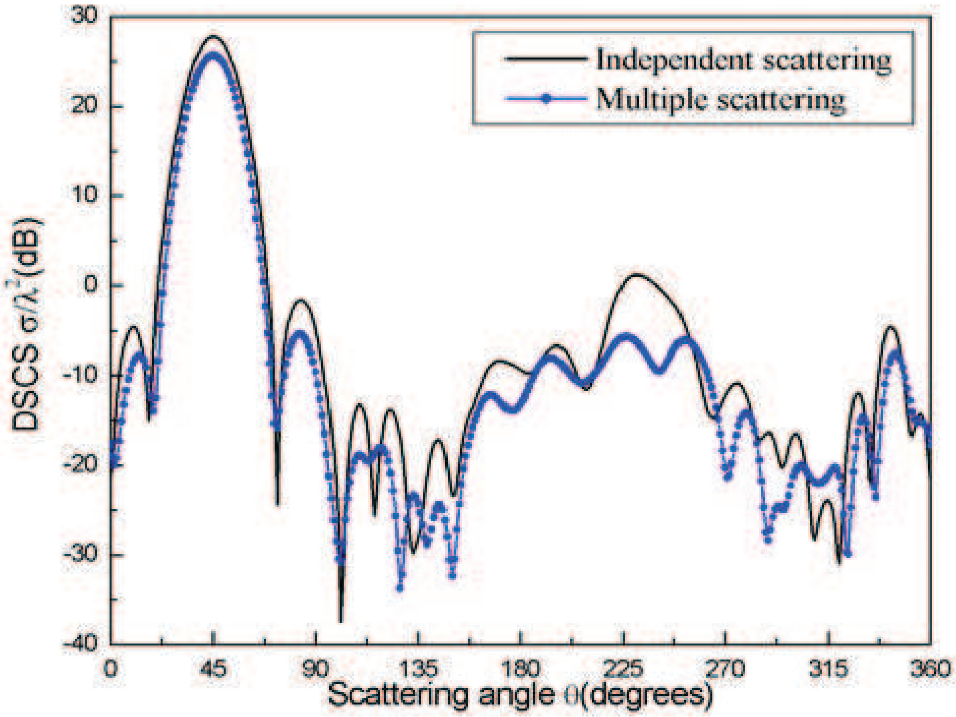

Figure 16. Comparison of the DSCS for the independent scattering and the multiple scattering: E-plane.

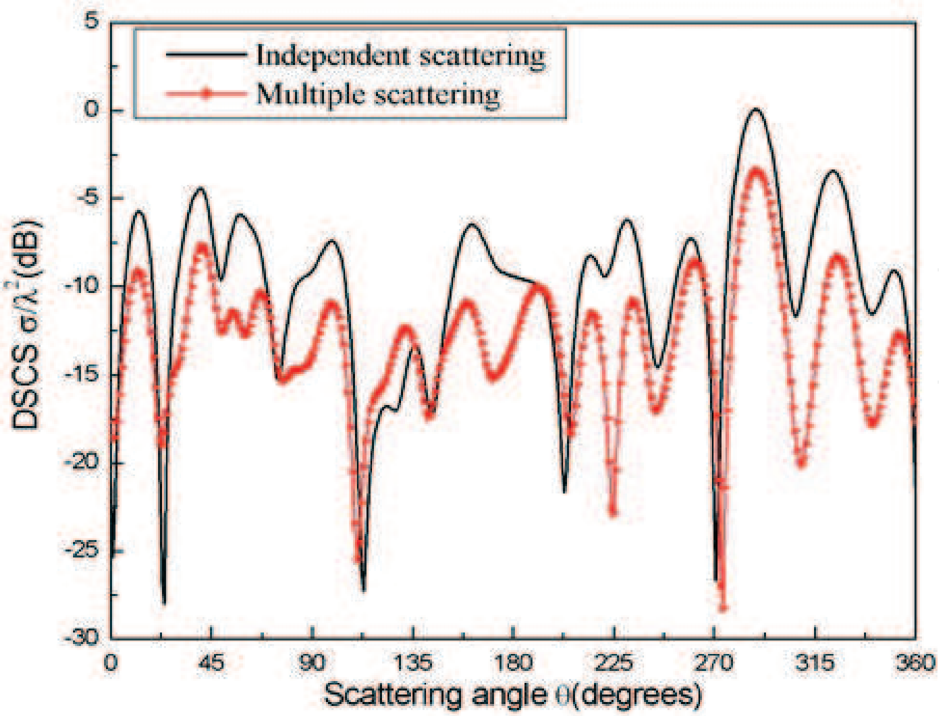

Figure 17. Comparison of the DSCS for the independent scattering and the multiple scattering: H-plane.

results show that the interactions of the particles lead to a reduction in the scattering intensities, which are identical to the general idea of scattering theory.

Author details

Yi Ping Han*, Zhi Wei Cui and Jia Jie Wang

*Address all correspondence to: yphan@xidian.edu.cn

School of Physics and Optoelectronic Engineering, Xidian University, China

References

[1] Gouesbet G and Onofri FRA. Preface: laser-light and interactions with particles (LIP), 2014. Journal of Quantitative Spectroscopy & Radiative Transfer. 2015;162:1–7.

[2] Mishechenko MI, Travis LD, and Lacis AA. Scattering, absorption, and emission of light by small particles. 2002, Cambridge: Cambridge University Press.

[3] Doicu A, Wriedt T, and Eremin YA. Light scattering by systems of particles null-field method with discrete sources: theory and programs. 2006, Berlin: Springer-Verlag.

[4] Gouesbet G and Gréhan G. Generalized Lorenz-Mie theories. 2011, Berlin: Springer.

[5] Lock JA and Gouesbet G. Rigorous justification of the localized approximation to the beam-shape coefficients in generalized Lorenz-Mie theory. I. On-axis beams. The Journal of the Optical Society of America A. 1994;11(9):2503–2515.

[6] Gouesbet G and Lock JA. Rigorous justification of the localized approximation to the beam-shape coefficients in generalized Lorenz-Mie theory. II. Off-axis beams. The Journal of the Optical Society of America A. 1994;11(9):2516–2525.

[7] Gouesbet G, Maheu B, and Grehan G. Light scattering from a sphere arbitrarily located in a Gaussian beam, using a Bromwich formulation. The Journal of the Optical Society of America A., 1988;5:1427–1443.

[8] Wang JJ, Gouesbet G, Han YP, and Grehan G. Study of scattering from a sphere with an eccentrically located spherical inclusion by generalized Lorenz-Mie theory: internal and external field distribution. The Journal of the Optical Society of America A. 2011;28:24–39.

[9] Han L, Han YP, Wang JJ, and Cui ZW. Internal and near-surface electromagnetic fields for a dielectric spheroid illuminated by a zero-order Bessel beam. Journal of the Optical Society of America a-Optics Image Science and Vision. 2014;31(9):1946–1955.

[10] Onofri F, Grehan G, and Gouesbet G. Electromagnetic scattering from a multilayered sphere located in an arbitrary beam. Applied Optics. 1995;30:7113–7124.

[11] Gouesbet G, Wang JJ, and Han YP. Transformations of spherical beam shape coefficients in generalized Lorenz-Mie theories through rotations of coordinate systems. I. General formulation. Optics Communication. 2010;283:3218–3225.

[12] Wang JJ, Gouesbet G, and Han YP. Transformations of spherical beam shape coefficients in generalized Lorenz-Mie theories through rotations of coordinate systems. II. Axisymmetric beams. Optics Communication. 2010;283:3226–3234.

[13] Gouesbet G, Lock JA, Wang JJ, and Grehan G. Transformations of spherical beam shape coefficients in generalized Lorenz-Mie theories through rotations of coordinate systems. V. Localized beam models. Optics Communication. 2011;284:411–417.

[14] Han YP, Zhang Y, Zhang HY, and Han GX. Scattering of typical particles by beam shape in oblique illumination. Journal of Quantitative Spectroscopy & Radiative Transfer. 2009;110:1375–1381.

[15] Edmonds AR. Angular momentum in quantum mechanics. 1957, Princeton: Princeton University Press.

[16] Asano S and Yamamoto G. Light scattering by a spheroid particle. Applied Optics. 1975;14:29–49.

[17] Barton JP. Internal and near-surface electromagnetic fields for a spheroidal particle with arbitrary illumination. Applied Optics. 1995;34:5542–5551.

[18] Barton JP. Internal, near-surface, and scattered electromagnetic fields for a layered spheroid with arbitrary illumination. Applied Optics. 2001;40(21):3598–3607.

[19] Barton JP. Electromagnetic fields for a spheroidal particle with an arbitrary embedded sources. The Journal of the Optical Society of America A. 2000;17:458–464.

[20] Yiping H and Zhensen W. The expansion coefficients of a spheroidal particle illuminated by Gaussian beam. IEEE Transactions on Antennas and Propagation. 2001;49(4): 615–620.

[21] Han YP, Grehan G, and Gouesbet G. Generalized Lorenz-Mie theory for a spheroidal particle with off-axis Gaussian-beam illumination. Applied Optics. 2003;42:6621–6629.

[22] Han YP, Mees L, Ren KF, Grehan G, Wu ZS, and Gouesbet G. Far scattered field from a spheroid under a femtosecond pulsed illumination in a generalized Lorenz-Mie theory framework. Optics Communication. 2004;231:71–77.

[23] Xu F, Ren KF, Gouesbet G, Grehan, and Cai X. Generalized Lorenz-Mie theory for an arbitrary oriented, located, and shaped beam scattered by homogeneous spheroid. The Journal of the Optical Society of America A. 2007;24:119–131.

[24] Xu F, Ren K, and Cai X. Expansion of an arbitrarily oriented, located, and shaped beam in spheroidal coordinates. The Journal of the Optical Society of America A. 2007;24 (1):109–118.

[25] Flammer C. Spheroidal wave functions. 1957, California: Stanford U.P.

[26] Cui ZW, Han YP, and Zhang HY. Scattering of an arbitrarily incident focused Gaussian beam by arbitrarily shaped dielectric particles. The Journal of the Optical Society of America B. 2011;28:2625–2632.

[27] Han YP, Cui ZW, and Gouesbet G. Numerical simulation of Gaussian beam scattering by complex particles of arbitrary shape and structure. Journal of Quantitative Spectroscopy & Radiative Transfer. 2012;113:1719–1727.

[28] Han YP, Cui ZW, and Zhao WJ. Scattering of Gaussian beam by arbitrarily shaped particles with multiple internal inclusions. Optics Express. 2012;20:718–731.

[29] Barton JP and Alexander DR. Fifth-order corrected electromagnetic fields components for a fundamental Gaussian beam. Journal of Applied Physics. 1989;66:2800–2802.

[30] Edmonds AR. Angular momentum in quantum mechanics. 1957, Princeton: Princeton University Press.

[31] Tsang L, Kong JA, Ding KH, and Ao CO. Scattering of electromagnetic waves, numerical simulations. 2001, New York: Wiley.

[32] Ishimaru A. Wave propagation and scattering in random media. 1978, New York: Academic.

[33] Foldy LL. The multiple scattering of waves. I. General theory of isotropic scattering by randomly distributed scatterers. Physical Review Letters. 1945;67:107–119.

[34] Lax M. Multiple scattering of waves. Reviews of Modern Physics. 1951;23:287–310.

[35] Varadan VV and Varadan VK. Multiple scattering of electromagnetic waves by randomly distributed and oriented dielectric scatters. Physical Review. 1980;21:388–394.

[36] Varadan VK, Bringi VN, Varadan VV, and Ishimaru A. Multiple scattering theory for waves in discrete random media and comparison with experiments. Radio Science. 1983;18:321–327.

[37] Furutsu K. Multiple scattering of waves in a medium of randomly distributed particles and derivation of the transport equation. Radio Science. 1975;10:29–44.

[38] Tsang L, Kong JA, and Ding KH. Scattering of electromagnetic waves, theories and applications. 2000, New York : Wiley.

[39] Tishkovets VP and Jockers K. Multiple scattering of light by densely packed random media of spherical particles: dense media vector radiative transfer equation. Journal of Quantitative Spectroscopy & Radiative Transfer. 2006;101:54–72.

[40] Lu CC, Chew WC, and Tsang L. The application of recursive aggregate T-matrix algorithm in the Monte Carlo simulations of the extinction rate of random distribution of particles. Radio Science. 1995;30:25–28.

[41] Chew WC, Lin JH, and Yang XG. An FFT T-matrix method for 3D microwave scattering solution from random discrete scatterers. Microwave and Optical Technology Letters. 1995;9:194–196.

[42] Siqueira PR and Sarabandi K. T-matrix determination of effective permittivity for three-dimensional dense random media. IEEE Transactions on Antennas and Propagation. 2000;48:317–327.

[43] Mishchenko MI, Liu L, Mackowski DW, Cairns B, and Videen G. Multiple scattering by random particulate media: exact 3D results. Optics Express. 2007;15:2822–2836.

[44] Chart CH and Tsang L. A sparse-matrix canonical-grid method for scattering by many scatterers. Microwave and Optical Technology Letters. 1995;8:114–118.

[45] Barrowes BE, Ao CO, Teixeira FL, and Kong JA. Sparse matrix/canonical grid method applied to 3-D dense medium simulations. IEEE Transactions on Antennas and Propagation. 2003;51:48–58.

[46] Cui ZW, Han YP, and Xu Q. Numerical simulation of multiple scattering by random discrete particles illuminated by Gaussian beams. The Journal of the Optical Society of America A. 2011;28:2200–2208.

[47] Sun YF, Chan CH, Mittra R, and Tsang L. Characteristic basis function method for solving large problem arising in dense medium scattering. IEEE Antennas and Propagation Society International Symposium. 2003;2:1068–1071.

[48] Mackowski DW and Mishchenko MI. Direct simulation of multiple scattering by discrete random media illuminated by Gaussian beams. Physical Review Letters A. 2011;83:013804.

[49] Cui ZW, Han YP, and Li CY. Simulation of electromagnetic scattering by random discrete particles using a hybrid FE-BI-CBFM technique. Waves Random Complex Media. 2012;22:207–221.

[50] Jin JM. The finite element method in electromagnetics. 2002, New York: Wiley.